Original Research Article

SCIENCE PROGRESS

Science Progress
2024, Vol. 107(4) 1–20

DOI: 10.1177/00368504241300855
journals.sagepub.com/home/sci
Sage

Optimal condition confirmation of treatment conditions through analysis of intratumoral apoptotic temperature range of microwave ablation for various microwave frequencies and antenna insertion depth

Donghyuk Kim and Hyunjung Kim
Department of Mechanical Engineering, Ajou University, Suwon, South Korea

Abstract
Microwave ablation is a therapeutic technique that kills tumors by inducing heat generation in biological tissue through microwave emissions. Microwave ablation is a minimally invasive treatment technique, which has the advantage of treating deeply located tumors with less bleeding than traditional surgical techniques. In this study, the therapeutic effect of microwave ablation was analyzed from the perspective of the temperature range where apoptosis and necrosis occur. Through the numerical modelling, the tumor located inside the liver tissue was implemented, and the temperature distribution in the hepatic tissue was calculated by varying value of the microwave frequency, microwave antenna input power, and the insertion depth of the microwave coaxial antenna. Microwave frequencies were selected as 915, and 2450 MHz, and the insertion depth of the microwave coaxial antenna was set at a distance difference between the tumor tip and the slot of 4 to 16 mm. In addition, the microwave antenna input power was set to a range of 0 to 60 W. Based on the obtained temperature distribution, the apoptotic variables, which are parameters specifically defined apoptosis ratios that can quantitatively verify the therapeutic effect, were calculated to derive the microwave ablation treatment condition that maximizes the therapeutic effect for each microwave frequency. Through the quantitative analysis of apoptotic variables, the optimal conditions for maximum therapeutic effect were derived for each microwave frequency analyzed in this study. For frequencies of 915 MHz, the optimal insertion depth of the antenna is 8 mm

Corresponding author:
Hyunjung Kim, Department of Mechanical Engineering, Ajou University, 206, World cup-ro, Yeongtong-gu, Suwon 16499, South Korea.
Email: hyunkim@ajou.ac.kr

above the bottom of the tumor, and the optimal microwave input power is 40 W. For 2450 MHz, the optimal insertion depth and input power were found to be 4 mm and 4 W, respectively. Ultimately, it is expected that the results presented in this study will lead to more improved treatment of microwave ablation in practice.

Keywords
Apoptosis, coaxial-slot antenna, insertion depth, microwave frequency, microwave ablation, thermal damage

Introduction

Cancerous tumors develop in a variety of locations in the human body. The medical practice uses a variety of methods to treat them. Currently, cancer treatment is performed in different ways, including traditional surgery, radiotherapy, chemotherapy, immunotherapy, and thermal ablation.[1–5] Since each has distinct advantages and disadvantages, an appropriate treatment method should be adapted to individual patient. Among them, the most commonly performed treatment technique is through the surgical removal, which is difficult to treat tumors that occur in deep parts of the body, and there is a risk of secondary infection because of bleeding.[6] To address these limitations, the medical field is constantly investigating various alternative treatments. Among them, microwave ablation (MWA) is a therapeutic technique that causes tumor damage by heating biological tissue through microwave emission.[7,8] MWA is a minimally invasive therapeutic technique, which has the advantage of causing less bleeding than traditional surgical techniques by making incisions. In addition, it has the advantage of treating tumors that occur in deep locations inside the human body.

MWA is a therapeutic technique that kills targeted tumors by raising their temperature. In biological tissues, there are two main mechanisms of cell death that are temperature dependent: apoptosis and necrosis.[9] Of the two, apoptosis is programmed cell death and involves the cell killing itself and it is known to occur for temperatures between 43 °C and 50 °C.

A number of studies have been conducted to analyze MWA through numerical analysis. Shamekhi et al.[10] analyzed the MWA effect according to various antenna types. The temperature distribution in the tissue was analyzed using three different coaxial antennas: single-slot, double-slot, and dipole-tip, as well as a new type of antenna called the micro-cut slot (MCS) antenna. Through theoretical and numerical analysis, the temperature distribution was determined for blood-perfused tissues consisting of normal and cancerous cells. As a result of the analysis, it was confirmed that a single-slot antenna shows high effectiveness for sphere and oval tumor types. Gas[11] analyzed the MWA effect of different numbers of slots inside multi-slot coaxial antenna structures using two-dimensional finite element analysis. The thermo-electrical characteristics of biological tissue were considered when the frequency 2.45 GHz was employed. MWA treatment was implemented for the brain, breast, kidney, liver, and lung tissues, and the steady-state temperature distribution and maximum temperature reached within each tissue by microwave antenna with different number of active slots were confirmed. Finally, it was found that there was no significant difference in the therapeutic effect as the number of slots increased, and the temperature decreased rapidly as the distance from the antenna increased. In addition, various researchers are numerically studying microwave ablation.[12,13]

Previous MWA studies based on numerical simulations have indirectly confirmed the therapeutic effect through calculations of electromagnetic absorption and temperature distribution. However, most articles simply analyzed the treatment effect based on a specific temperature without information on apoptosis and necrosis, which are commonly used in the biological field, and did not provide a quantitative treatment effect, and the amount of thermal damage to surrounding normal tissue during the treatment progressed. Therefore, in this study, MWA therapeutic effects were quantitatively analyzed by examining the relationship between apoptosis and necrosis. Through the apoptotic variable proposed by Kim and Kim,[14] the degree of intratumoral apoptosis and the amount of thermal damage to surrounding normal tissues were identified, and the therapeutic effects of various microwave frequencies and insertion depth of microwave coaxial antenna (MCA) were analyzed. Moreover, information on the MCA insertion depth and microwave input power with the optimal therapeutic effect for each microwave frequency is finally presented.

Materials and methods

Analysis of electromagnetic wave emission behavior in biological tissue

In this study, the wave equation was used to analyze the electromagnetic wave emission behavior of MCA inserted in biological tissues. The electromagnetic waves emitted by the MCA are characterized by transverse electromagnetic fields, and the electric field ($\vec{E}$) and magnetic field ($\vec{H}$) can be expressed as the following equations:[15]

$$\vec{E} = \overrightarrow{\mathrm{e}_r} \frac{C}{r} e^{\mathrm{j}(\omega t - k_\mathrm{p} z)} \tag{1}$$

$$\vec{H} = \overrightarrow{\mathrm{e}_\varphi} \frac{C}{rZ} e^{\mathrm{j}(\omega t - k_\mathrm{p} z)} \tag{2}$$

$$C = \sqrt{\frac{ZP_\mathrm{in}}{\pi \cdot ln\left(\frac{r_\mathrm{outer}}{r_\mathrm{inner}}\right)}} \tag{3}$$

$$\omega = 2\pi f, \qquad k_\mathrm{p} = \frac{2\pi}{\lambda} \tag{4}$$

where Z, P_in, and r are the wave impedance, microwave input power, and radial coordinate, respectively, and ω, f, k_p, and λ are the angular frequency, frequency, propagation constant, and wavelength, respectively.

As the magnetic field is only present in the azimuthal direction, the modelling of MCA used the wave formulation of axisymmetric transverse magnetic fields under axial symmetry conditions. Thus, the final wave equation in axisymmetrical can be written in terms of the H_φ component as follows:[15]

$$\nabla \times \left(\left(\varepsilon_r - \frac{j\sigma}{\omega \varepsilon_0} \right)^{-1} \nabla \times H_\varphi \right) - \mu_r \frac{\omega^2}{c_0^2} H_\varphi = 0 \tag{5}$$

where ϵ_r and ϵ_0 are relative permittivity and vacuum permittivity (8.854×10^{-12} F/m), respectively, and σ, μ_r, and c_0 are electrical conductivity, relative permeability, and speed of light in vacuum, respectively.

The boundary condition of the MCA surface is set as equation (6), assuming a perfect electric conductor, and scattering boundary condition of equation (7) is applied to the end surface of the biological tissue, namely[11]:

$$\hat{n} \times \vec{E} = 0 \tag{6}$$

$$\hat{n} \times \sqrt{\varepsilon}\vec{E} - \sqrt{\mu}\,\vec{H} = -2\sqrt{\mu}\,H_{\varphi 0}\overrightarrow{e_\varphi} \quad \left(H_{\varphi 0} = \frac{C}{Zr} \right) \tag{7}$$

The boundary condition of the MCA surface is set as equation (6), assuming a perfect electric conductor, and scattering boundary condition of equation (7) is applied to the end surface of the biological tissue. Type of port was set to coaxial, and for port mode, transverse electromagnetic mode was used.

For electrical properties, it has characteristics that vary with temperature and microwave frequency.[16] In this study, frequencies of 915 and 2450 MHz were selected, and different equations were applied for the liver and tumor.[16–19] First, for relative permittivity, properties at the corresponding temperature range can be calculated for each frequency as shown in the following equations:

$$\varepsilon_{r,\mathrm{liver},915\,\mathrm{MHz}}(T) \begin{cases} 0.072T + 48.64 & 30 \le T \le 95\ ^\circ\mathrm{C} \\ -3.40T + 370 & 95 \le T \le 100\ ^\circ\mathrm{C} \\ 30 & 100\ ^\circ\mathrm{C} \le T \end{cases} \tag{8}$$

$$\varepsilon_{r,\mathrm{liver},2450\,\mathrm{MHz}}(T) \begin{cases} -0.042(T + 273.15) + 47.043 & 37 \le T \le 100\ ^\circ\mathrm{C} \\ -14.55(T + 273.15) + 5459.8 & 100 \le T \le 101\ ^\circ\mathrm{C} \\ 16.67 & 101\ ^\circ\mathrm{C} \le T \end{cases} \tag{9}$$

$$\varepsilon_{r,\mathrm{tumor},2450\,\mathrm{MHz}}(T) \begin{cases} 48.16 & 37 \le T \le 100\ ^\circ\mathrm{C} \\ 24.08 & 100\ ^\circ\mathrm{C} < T \end{cases} \tag{10}$$

For tumors at 915 MHz, the average relative permittivity obtained from in vivo experiments, 64.09, proposed by O'Rourke et al.,[20] was applied due to the lack of research.

Electrical conductivity also applied different equations depending on the microwave frequency, as shown in the following equations:

$$\sigma_{\mathrm{liver},915\,\mathrm{MHz}}(T) \begin{cases} 0.00897T + 0.5282 & 30 \le T \le 95\ ^\circ\mathrm{C} \\ -0.0512T + 6.244 & 95 \le T \le 100\ ^\circ\mathrm{C} \\ 0.2 & 100\ ^\circ\mathrm{C} \le T \end{cases} \tag{11}$$

$$\sigma_{\text{liver,2450 MHz}}(T)\begin{cases} -0.0004(T+273.15)+1.7381 & 37 \le T \le 100\ ^\circ\text{C} \\ -0.78(T+273.15)+294.17 & 100 \le T \le 101\ ^\circ\text{C} \\ 0.81 & 101\ ^\circ\text{C} \le T \end{cases} \tag{12}$$

$$\sigma_{\text{tumor,2450 MHz}}(T)\begin{cases} 2.09 & 37 \le T \le 100\ ^\circ\text{C} \\ 1.05 & 100\ ^\circ\text{C} < T \end{cases} \tag{13}$$

For the tumor at 915 MHz, the average electrical conductivity of 1.34 S/m obtained from in vivo experiments proposed by O'Rourke et al.[20] was applied.

For the electrical properties of the components of the MCA, the values were taken from previous studies.[11,21,22]

Analysis of thermal behavior in biological tissue

Microwave emission from the MCA leads to a temperature increase in the tissue. Therefore, the Pennes bioheat equation (equation (14)) was used to analyze the thermal behavior inside biological tissues.[23] The equation considers the amount of heat transferred by blood flow and metabolism and the amount of heat transferred by the microwave, namely[24]:

$$\rho c_p \frac{\partial T}{\partial t} = \nabla \cdot (k_m \nabla T) + \rho_b c_{p,b} \omega_b (T_b - T) + Q_{met} + Q_{mw} \tag{14}$$

$$Q_{mw} = \rho \text{SAR}, \qquad \text{SAR} = \frac{\sigma}{2\rho} |\vec{E}|^2 \tag{15}$$

where ρ, c_p, T, and t represent density, specific heat, temperature, and time, respectively, and k_m, ω_b, and Q_{met} represent the thermal conductivity of tissue, blood perfusion rate, and heat generation by metabolism, respectively. In this study, ρ_b, $c_{p,b}$, and ω_b were set to 1060 kg/m^3, 3600 J/kg/K, and 0.015 1/s, respectively, and Q_{met} was set to 33,800 W/m^3.[15,21]

The amount of heat transferred by a microwave is expressed as Q_{mw}, which can be calculated from the density of the tissue and the specific absorption rate (SAR) (equation (15)), where SAR is calculated from the electrical conductivity of the medium, density, and the strength of the electric field.

Thermal properties of liver tissue also have characteristics that change depending on temperature, as shown in the following equations:[25–28]

$$W_a(T) = \begin{cases} -0.779e^{\left(\frac{T-106}{3.42}\right)} + 0.778 & T \le 103\ ^\circ\text{C} \\ -0.03924(T-103) + 0.454392 & 103 \le T \le 104\ ^\circ\text{C} \\ 0.778e^{\left(-\frac{T-80}{34.37}\right)} & 104\ ^\circ\text{C} \le T \end{cases} \tag{16}$$

$$\rho_{\text{liver}}(T) = -300W_a(T) + 1300 \tag{17}$$

$$c_{p,\text{liver}}(T) = 4190[0.63W_a(T) + 0.37] \tag{18}$$

$$k_{m,\text{ iver}}(T) = 0.419[1.36W_a(T) + 0.133] \tag{19}$$

For tumor, it was assumed that the thermal properties do not change with temperature and were fixed at a single value.[22] The density, specific heat, and thermal conductivity of the tumor were set to 1040 kg/m^3, 3960 J/kg/K, and 0.57 W/m/K, respectively.[12,22]

Numerical conditions

This study analyzed the MWA of tumors developed inside the liver tissue through numerical analysis. Figure 1 shows a schematic diagram of the numerical model. It was assumed that a spherical tumor with a radius of 10 mm developed at 40 mm from the upper boundary of rectangular piece of liver tissue with a radius and depth of 40 and 80 mm, respectively. The MCA consists of a catheter, conductor, dielectric, and slot, and was assumed to be inserted into the central z-axis of the tumor. The slot was set to be 3 mm above the tip of the MCA, and slot length was set to 1 mm. The numerical analysis was performed by varying the insertion depth of the MCA (d_m) based on the bottom end of the slot.

Finally, in this study, the effect of MWA on different microwave frequencies (f) and insertion depths of MCA (d_m) was quantitatively verified. Accordingly, f was set to 915, and 2450 MHz, respectively, and d_m was set in four steps from 4 to 16 mm based on the position of the bottom edge of the slot and the bottom boundary of the tumor. The heating time was fixed at 300 seconds, and the microwave input power (P_{in}) was set in 61 steps from 0 to 60 W. Table 1 summarizes all numerical conditions. In all considered cases, the

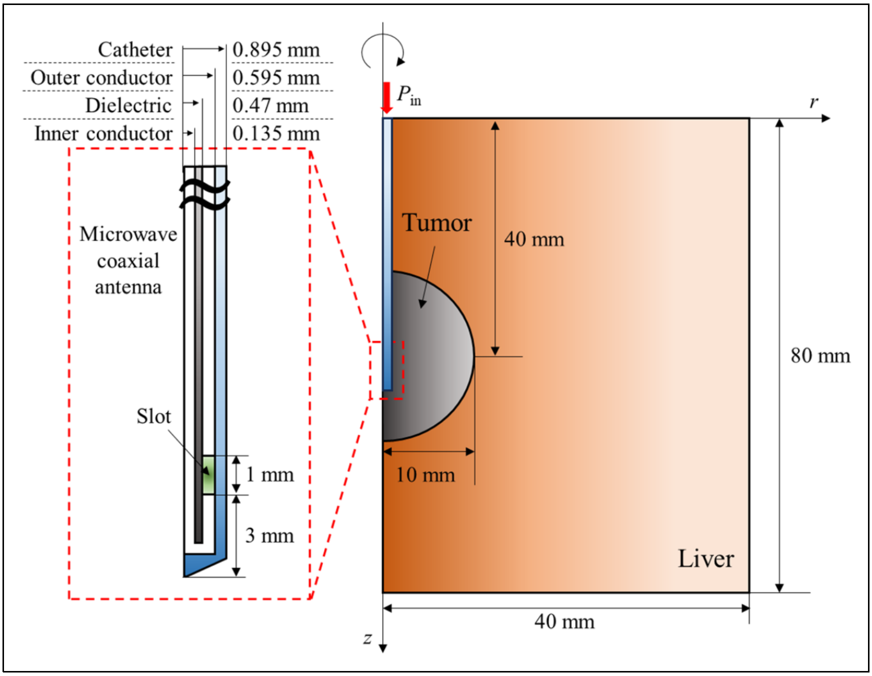

Figure 1. Schematic view of numerical model.

Table 1. Parameters of numerical analysis.

Parameter	Case	Iteration number	Step value
Microwave antenna input power (P_{in})	0–60 W	61	1 W
Microwave frequency (f)	915, 2450 MHz	2	
MCA insertion depth (d_m)	4–16 mm	4	4 mm

therapeutic effect of MWA was quantitatively investigated by observing the electromagnetic and temperature behavior inside the hepatic tissue, and the conditions that produce the optimal therapeutic effect for each working frequency were suggested.

Results and discussion

Validation of numerical simulation

First, to validate the numerical modeling, comparison, and verification with the results of Yang et al.[27] were performed. The verification model was set to insert an MCA with a radius of 1.25 mm into the center of liver tissue with a length and radius of 40 mm, as shown in Figure 2.

A plastic template and a plastic cutting board were placed at the top and bottom, respectively, and the ends of each component were set to be surrounded by air. Ex vivo experiments were performed, and liver tissues were kept refrigerated for one day so the initial temperature of the liver was set at 8 °C, and ambient temperature was set at 25 °C. The microwave power and frequency were set at 75 W and 2450 MHz, respectively.

Figure 3 shows a graph comparing the results of Yang et al.[27] with the results obtained by the numerical model presented in this study. The temperature change at 4.5 and 9 mm from the center of the slot was compared. The results were compared with previous studies over a heating time of 150 seconds, and the average RMSE at two points was derived as 3.5%. Checking the error at each point as a percentage, the error at the 4.5 and 9 mm points came out to be about 5.6% and 5.4%, respectively. This is because various biological phenomena, such as protein denaturation during steep temperature increases, are not applied for in the model. However, except for the first 50 seconds, the averages of RMSE and error percentage decrease to 2.7%, respectively, and through this, it was judged that the model in this study well reflects the actual phenomenon.

Microwave power absorbed in biological tissue

Prior to analyzing the quantitative therapeutic effects of MWA, the degree of microwave power absorption in the medium for each f and d_m parameter was determined. Figure 4 shows the absorption of microwave power in biological tissue for different frequencies.

Figure 4(a) and (c) are the power deposition distribution of biological tissue, and Figure 4(b) and (d) are the dB distribution from the maximum value. The MCA was

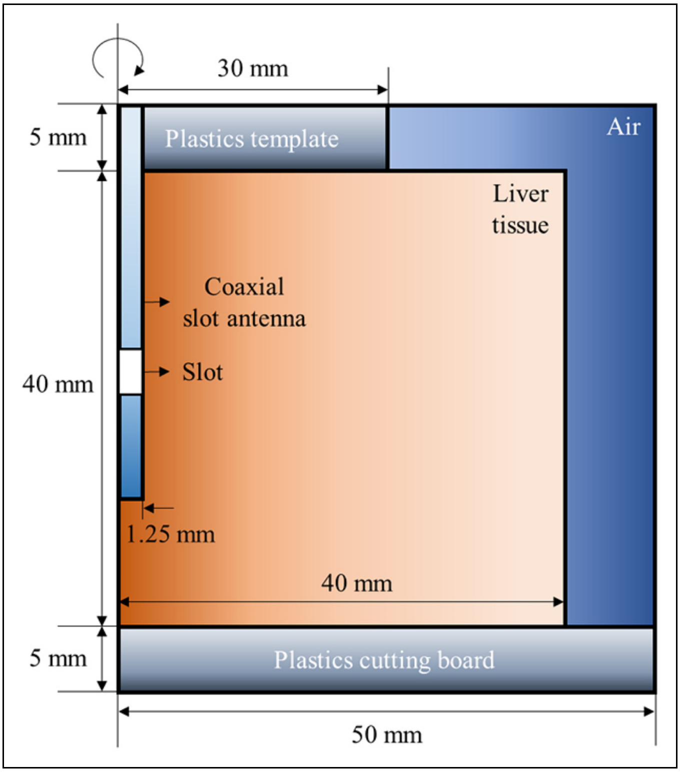

Figure 2. Schematic view of validation numerical model.

inserted at a point 8 mm from the bottom boundary of the tumor based on the bottom edge of the slot, and 30 W was applied for microwave antenna input power. In the graph, the white circle inside represents the tumor. As shown, applied frequency determines the area and degree of absorption of microwave power in the medium. When $f = 915$ MHz (Figure 4(a)), the center part of the tumor, which is the near part of the MCA, absorbs microwave power, and when $f = 2450$ MHz (Figure 4(b)), the nearly entire tumor absorbs microwave power.

Figure 5 shows the absorption of microwave power in liver tissues as a function of insertion depth (d_m) when $f = 915$ MHz and P_{in} is 30 W. Figure 5(a) and (c) are the power deposition distribution of biological tissue, and Figure 5(b) and (d) are the dB distribution from the maximum value. The position of the slot is fixed at a point 3 mm from the tip of the MCA, so that for each d_m, the absorption range of microwave power in the tissue is different. Since the absorption amount and range of microwave power are closely related to the temperature distribution inside the tumor, the temperature inside the tumor can be maintained at the target temperature only by adjusting the appropriate P_{in} and MCA insertion depth for each f.

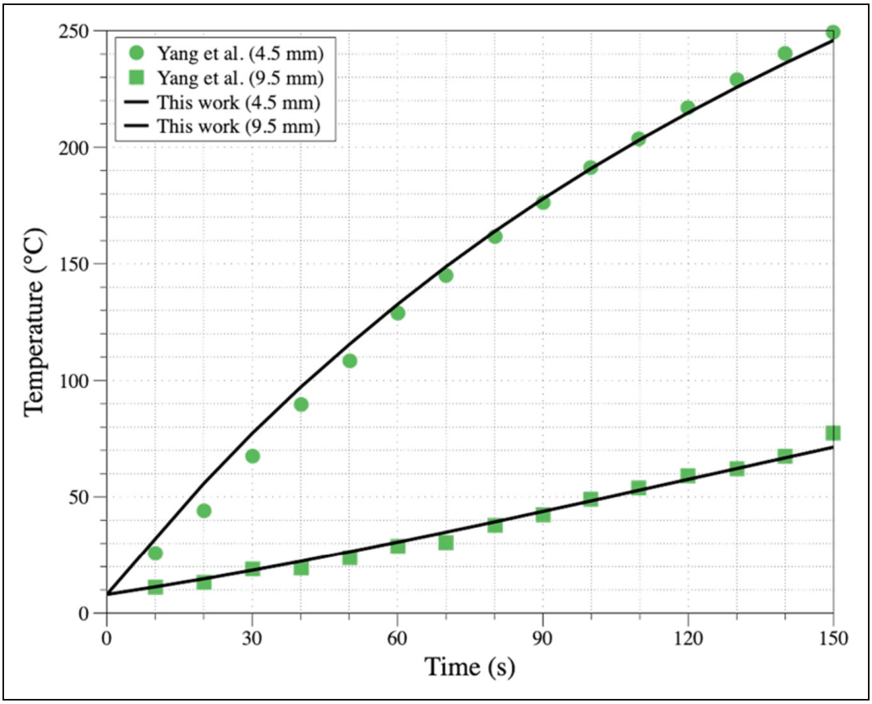

Figure 3. Validation of obtained result.

Temperature distribution in biological tissue

In the previous section, the absorption range and amount of microwave power inside liver tissues for different f and d_m parameters were identified. This leads to an increase in temperature inside the tissue. In the case of MCA, heating begins around the slot at the tip. This necessarily requires the MCA to be placed inside the tumor rather than on the edge of the tumor to heat more of the tumor area. This is because heat transfer generally occurs radially rather than in a specific direction. However, the area heated around the MCA varies with microwave frequency, and the insertion depth must be selected to account for this. In practical application, clinicians usually place the antenna at the edge of the tumor to avoid peripheral tumor infiltration. However, the main goal of this study is to set the tumor area as the target area and confirm whether the temperature increase distribution is calculated properly. So for each case, the temperature distribution of the tumor and surrounding liver tissue was confirmed. As this study analyzed the treatment effect based on the temperature range of apoptosis and necrosis, the temperature distribution in the tissue was also divided into these ranges.

Figure 6 shows the temperature distribution in biological tissue for different frequencies, when $d_m = 8$ mm and $P_m = 30$ W. The area inside the white line represents the tumor. As shown in this figure, for the same P_{in} values applied, the temperature distribution inside the tumor is different depending on the applied frequency. For lower

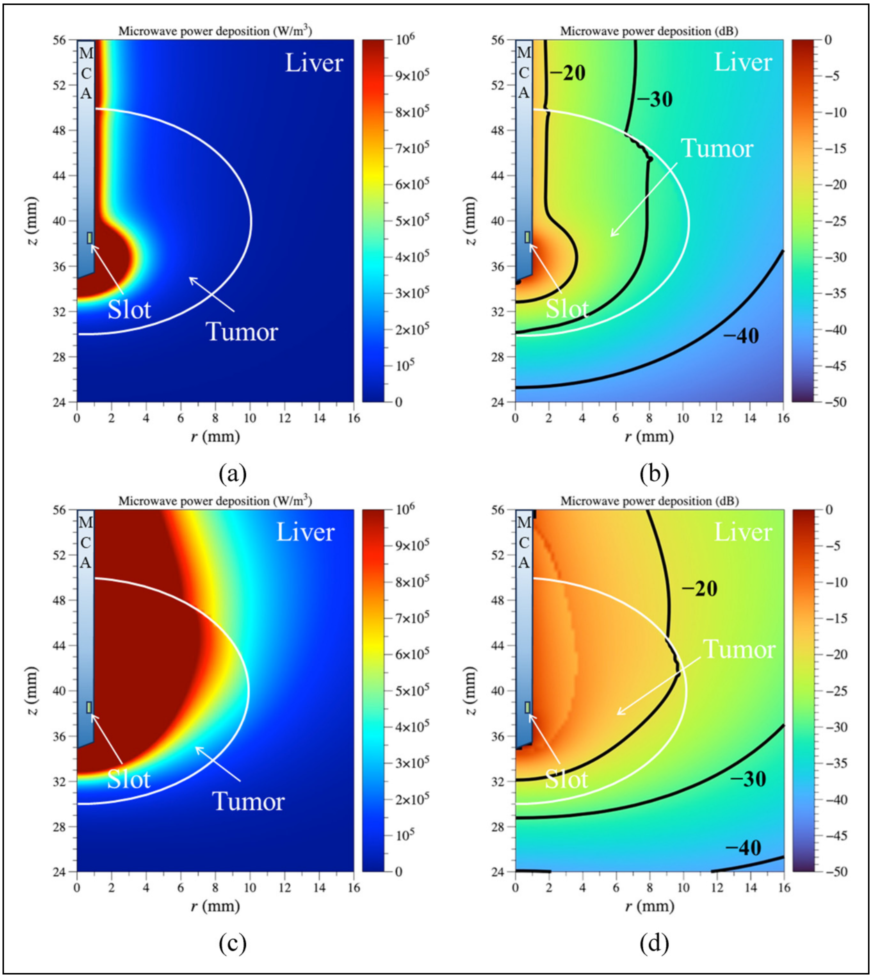

Figure 4. Microwave power deposition in tissues for various frequencies ($d_m = 8$ mm, $P_{in} = 30$ W, $t = 300$ s): (a) $f = 915$ MHz, power deposition, (b) $f = 915$ MHz, dB from maximum value, (c) $f = 2450$ MHz, power deposition, and (d) $f = 2450$ MHz, dB from maximum value.

frequencies (Figure 6(a)), only the region close to the MCA increases the temperature of the tumor to the necrosis region, and it was confirmed that 60% of the entire tumor area corresponded to the apoptosis temperature range. On the other hand, when $f = 2450$ MHz (Figure 6(b)), all areas within the tumor are elevated to the temperature range where necrosis occurs, and the surrounding liver tissue is also elevated to the necrosis temperature region. This leads to excessive thermal damage, so an appropriate value of f and P_{in} parameters should be given to increase the effectiveness of the treatment.

Figure 7 shows the temperature distribution in the liver tissue as a function of d_m when f is 915 MHz and P_{in} is 30 W. If MCA insertion depth is low (Figure 7(a)), the

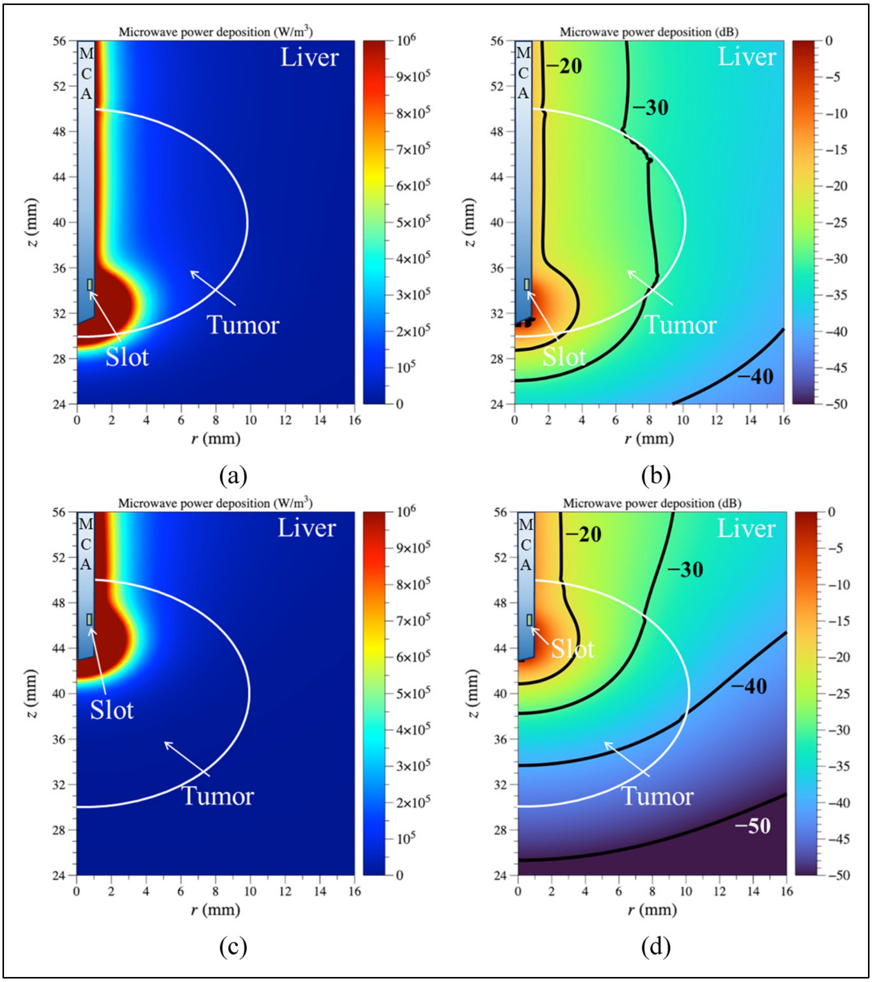

Figure 5. Microwave power deposition in tissues for various insertion depth values d_m ($f = 915$ MHz, $P_{in} = 30$ W, $t = 300$ s): (a) $d_m = 4$ mm, power deposition, (b) $d_m = 4$ mm, dB from maximum value, (c) $d_m = 16$ mm, power deposition, and (d) $d_m = 16$ mm, dB from maximum value.

temperature of the lower part of the tumor enters the necrosis region, but most of the tissue is in the apoptosis temperature range, which is the target temperature. In this case, it was confirmed that 56% of the tumor entered the apoptosis temperature range. However, the temperature of the liver tissue at the bottom and top of the tumor is also in the apoptosis and necrosis temperature range, so this is considered thermal damage and P_{in} should be reduced. On the other hand, if d_m is increased to 16 mm (Figure 7(b)), the temperature of the top part of the tumor contains the necrosis temperature range, and the apoptosis temperature range corresponds to 26%. For the lower part of the tumor, the temperature will not rise to the target temperature and will remain in the

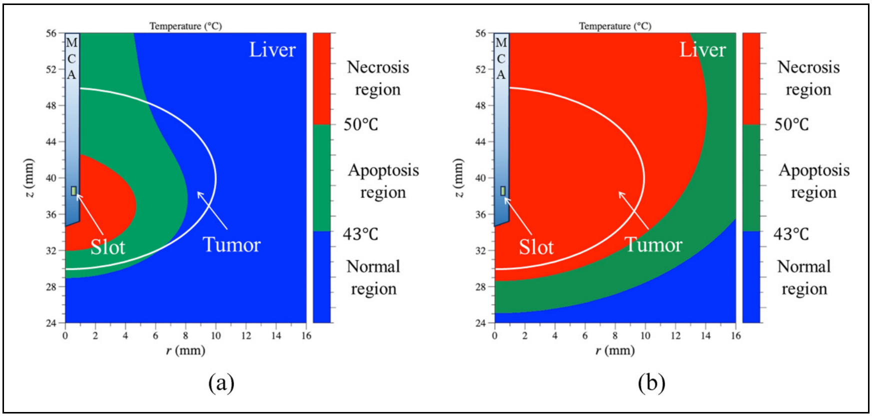

Figure 6. Temperature distribution for various frequencies ($d_m = 8$ mm, $P_{in} = 30$ W, $t = 300$ s): (a) $f = 915$ MHz and (b) $f = 2450$ MHz.

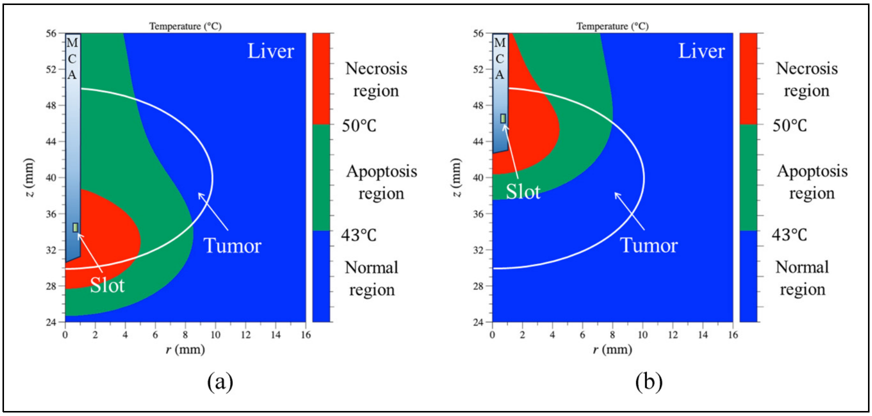

Figure 7. Temperature distribution for various insertion depth values d_m ($f = 915$ MHz, $P_{in} = 30$ W, $t = 300$ s): (a) $d_m = 4$ mm and (b) $d_m = 16$ mm.

normal range. The temperature of the liver tissue at the top of the tumor will also rise to the apoptosis and necrosis temperature range, causing thermal damage. However, from a heat transfer perspective, it is believed that if P_{in} is appropriately regulated, conditions exist within the tumor tissue to raise it to the apoptosis temperature range while the surrounding liver tissue remains in the normal range.

Based on these considerations, in this study, temperature distributions inside the tissue according to different P_{in} and d_m parameters were calculated for each frequency, and the regions corresponding to the apoptosis and necrosis temperature range of the tumor and surrounding normal tissue were quantitatively analyzed in all cases.

Apoptosis temperature distribution in tumor tissue

Various models have been proposed to determine cell death, such as the Arrhenius damage model.[29,30] Among various studies, Tehrani et al.[29] analyzed using three-state model of cell death. However, The study did not reflect thermophysical properties that change depending on temperature. Additionally, quantitative thermal damage to surrounding normal tissues was not presented. Accordingly, in this study, the apoptotic variable proposed by Kim et al.[14] was used to analyze quantitatively the degree and range of maintenance of apoptotic temperature range in tumor tissue. Among the three apoptotic variables, the apoptosis retention ratio ($\theta*_{A}$), which quantitatively determines the degree to which the temperature inside the tumor maintains the apoptotic temperature range, is defined as the ratio of the volume of the tumor to the volume corresponding to the apoptotic temperature range as shown in the following equation:

$$\theta^{*}_{\mathrm{A}} = \frac{1}{t}\int_{0}^{t} \frac{\mathit{Apoptotic\ volume}\ (\mathit{if}\ 43 < V_t(T) < 50}{\mathit{Total\ tumor\ volume}}\,dt \tag{20}$$

It ranges from 0 to 1, with a value of 1 indicating that $\theta*_{A}$ maintains the apoptotic temperature range for the total treatment time at all ranges within the tumor.

Figure 8 shows $\theta*_{A}$ distributions as a function of P_{in} and d_m parameters for different frequencies. When analyzing the maintenance of apoptosis temperature in the liver tumor, it was found that for each f and d_m, there exists a P_{in} value at which $\theta*_{A}$ is maximized. For a frequency of 915 MHz, $\theta*_{A}$ is maximized when d_m is 8 mm. In the low-frequency case, the absorption of microwave power is dominated at the bottom part of the tumor compared to the radial side of the MCA. As a result, heating occurs primarily in the lower tumor region of the MCA, so when d_m has a low value, only the lower region of the tumor maintains the apoptotic temperature. On the other hand, when d_m has a higher value of 16 mm, the heating occurs mainly in the upper part of the tumor, so the lower

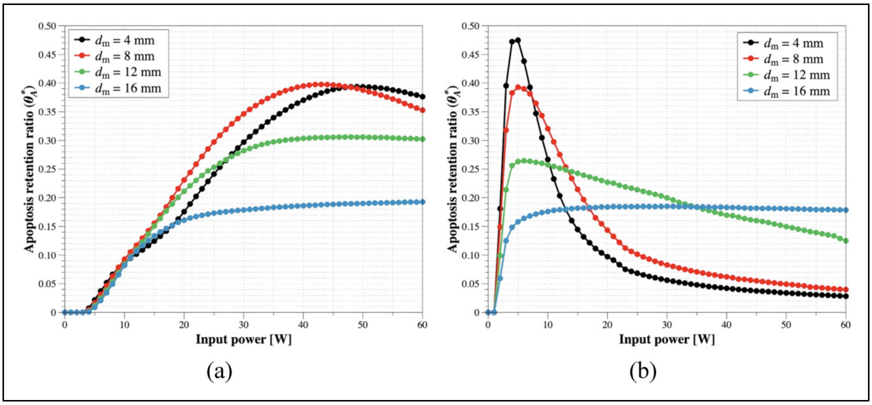

Figure 8. Apoptosis retention ratio ($\theta*_{A}$) distributions for various insertion depth values (d_m): (a) $f = 915$ MHz and (b) $f = 2450$ MHz.

part does not have an adequate temperature rise, resulting in a lower maximum parameter value of θ^*_A. For $f = 2450$ MHz, the maximum of θ^*_A is obtained when $d_m = 4$ mm. In this case, heat generation occurs over a larger radial area than for other frequencies, and the lower part of the MCA absorbs a relatively small amount of microwave antenna input power. As a result, when d_m increases, the bottom of the MCA generates less heat compared to the radial direction, requiring more P_{in} to reach the target temperature. However, in the upper part of the tumor, the temperature rises beyond the apoptosis temperature range to the temperature range where necrosis occurs. For this reason, the d_m value should be reduced to cause an appropriate temperature rise across the entire range of the tumor.

Thermal damage to surrounding normal tissue

During the MWA procedure, MCA is inserted into the tumor site, raising the temperature of the tumor tissue to perform the treatment. In the treatment process, the temperature increment occurs not only in the tumor tissue, but also in the surrounding normal tissue. This has the potential to cause unnecessary thermal damage to healthy tissue. For tumor tissue, the apoptotic temperature range is the target temperature range for treatment, but for normal tissue, this is also thermal damage, and different criteria should be applied to the surrounding normal tissue. To confirm the amount of thermal damage, the Arrhenius model is mainly used.[31] In this study, the thermal hazard retention value (θ^*_H) was used to analyze the amount of thermal damage to the surrounding normal tissue during treatment, quantitatively.[14] θ^*_H parameter is defined as the ratio of the weighted sum of normal tissue around the tumor, after weighting for biological phenomena occurring in each temperature range as shown in the following equation:

$$\theta^*_{\mathrm{H}} = \frac{1}{t}\int_0^t \frac{\sum_{\mathrm{j}=1}^{m} V_{n,t}(T)\cdot w_{\mathrm{j}}}{V_{n,t}}\,dt \tag{21}$$

For the calculated normal tissue area, up to 50% of the length was used based on the radius of the tumor tissue. This allows for quantitative analysis of the amount of thermal damage to surrounding normal tissue that occurs during MWA treatment.

Figure 9 shows θ^*_H distributions as a function of P_{in} and d_m parameters for various frequencies. In general, as employed frequency increases, θ^*_H rises for the same P_{in}. This is because as frequency increases, more microwave power is absorbed, resulting in increased heat generation in the surrounding normal tissue and increased heat transfer to the tumor tissue. θ^*_H increases as d_m value decreases for $f = 2450$ MHz. This is because as d_m decreases, heat generation occurs in the lower part of the MCA, which leads to heat generation in the normal tissue below the tumor, causing thermal damage. However, this trend will depend on the range over which θ^*_H is calculated. In this study, θ^*_H was calculated for normal tissue from the tumor tip to 50% length of the tumor radius. This is to calculate the amount of thermal damage only to normal tissue around the tumor and does not calculate the amount of thermal damage to normal tissue outside the applicable range. As d_m increases, the temperature of the

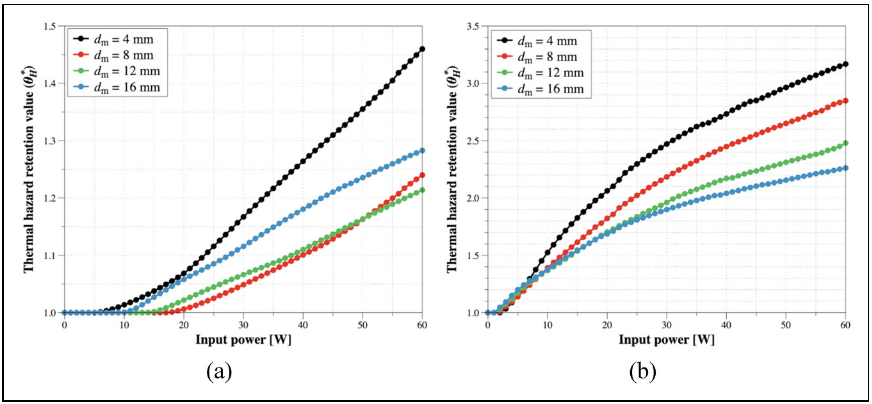

Figure 9. Thermal hazard retention value (θ^*_H) for various insertion depth values (d_m): (a) $f =$ 915 MHz and (b) $f = 2450$ MHz.

liver tissue above the tumor is expected to increase at 2450 MHz, and if the calculation range of θ^*_H is expanded, the trend of θ^*_H according to d_m is judged to change.

Confirmation of treatment effect and optimal treatment condition

During MWA, heating occurs simultaneously in the tumor and normal tissues. Also, the goal of the treatment is to destroy only the tumor cells, so conditions must be found that maximize the death of the cancerous cells while minimizing thermal damage to the surrounding normal tissue cells. Therefore, the effective apoptosis retention ratio (θ^*_{eff}) was used in this study to optimize these conditions.[14] The θ^*_{eff} parameter is calculated as the ratio of θ^*_A and θ^*_H as shown in the following equation:

$$\theta^*_{eff} = \frac{\theta^*_A}{\theta^*_H} \quad (22)$$

By calculating the θ^*_{eff} value in all cases, the therapeutic effect was quantitatively confirmed and the conditions that produce the optimal treatment effect were suggested.

Figure 10 shows θ^*_{eff} distributions as a function of P_{in} and d_m parameters for different frequencies. Note that θ^*_{eff} value is calculated as the ratio of θ^*_A to θ^*_H, so the trend of the result is similar to θ^*_A parameter. Analyzing all considered cases, it was found that for each frequency, there exists a d_m and P_{in} values with optimal MWA treatment effect. Comparing with the results for θ^*_A, for each f and d_m parameters, P_{in} at which θ^*_A maximizes decreases compared to the P_{in} at which θ^*_{eff} maximizes. This is because, from θ^*_{eff} optimal condition perspective, it is more beneficial to reduce thermal damage to surrounding normal tissue even if the apoptotic temperature within the tumor tissue is maintained lower. To achieve this, the amount of thermal damage to surrounding normal tissues must be reduced by reducing the P_{in}. In addition, the optimal value of θ^*_{eff} is lower compared to the optimal value of θ^*_A. This is because even if the temperature inside the tumor is maintained at the maximum apoptosis temperature, thermal damage

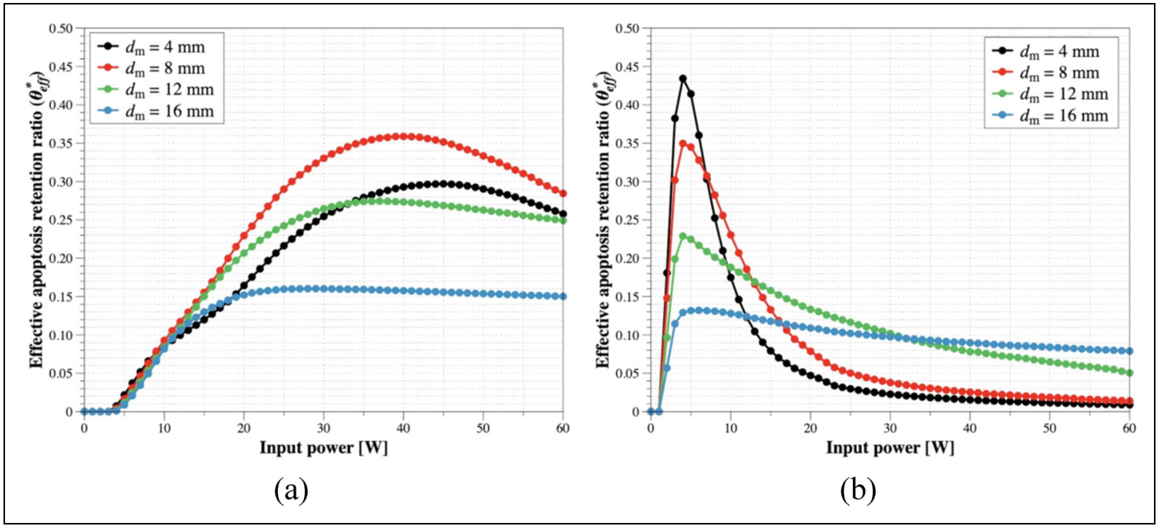

Figure 10. Effective apoptosis retention ratio (θ^*_{eff}) for various insertion depth values (d_{m}): (a) $f = 915$ MHz and (b) $f = 2450$ MHz.

Table 2. Optimal conditions for various values of microwave frequency.

f (MHz)	d_m (mm)	P_{in} (W)	θ^*_{eff}
915	8	40	0.359
2450	4	4	0.434

to the surrounding normal tissue is inevitable, and the optimal value of θ^*_{eff} is lowered to account for this. Finally, for $f = 915$ MHz, the MCA insertion position at 8 mm above the bottom boundary of the tumor was found to have the greatest therapeutic effect, and for $f = 2450$ MHz, the MCA insertion position at 4 mm was found to have the greatest therapeutic effect. The optimal treatment conditions for each frequency are summarized in Table 2. This allows us to determine the optimal treatment conditions for different microwave frequencies and MCA insertion depths.

Conclusions

In this study, the therapeutic effect of MWA on tumors developed inside the liver was analyzed numerically. The situation where MCA was injected into the tumor center axis was implemented with a numerical analysis model, and the distribution of electromagnetic field emitted by MCA was analyzed using the wave equation, and the temperature distribution was analyzed using the Pennes bioheat equation.

The numerical analysis was performed by varying the microwave frequency, MCA injection position, and microwave input power. After analyzing the treatment effect in all cases, the results showed that for microwave frequencies of 915 MHz, the MCA was inserted at a point 8 mm above the bottom of the tumor, and for 2450 MHz, the MCA was inserted at a point 4 mm above the bottom of the tumor for achieving maximum therapeutic effect. Based on the results of this study, it is believed that unnecessary thermal damage can be reduced by further reducing the margin in microwave ablation, which is currently treated with a certain margin. In addition, it is expected that the model can be used to identify conditions that deviate significantly from appropriate treatment conditions, thus avoiding the need to validate unnecessary conditions through experimental or clinical processes. However, since this study was based on numerical analysis, it will be useful for the confirmation of the numerical results that experimental measurements are carried out for the treatment conditions proposed in this study. In addition, this study did not consider water cooling to cool the MCA, but only tissue heating through microwave emission. Therefore, it is expected that higher input power is required to apply the results of this study to actual treatment.

Authors contributions

Donghyuk Kim: conceptualization, data curation, formal analysis, investigation, methodology, software, validation, visualization, writing–original draft, and writing–review and editing. Hyunjung Kim: conceptualization, funding acquisition, project administration, resources, supervision, and writing–review and editing.

Declaration of conflicting interests

The author(s) declared no potential conflicts of interest with respect to the research, authorship, and/or publication of this article.

Funding

The author(s) disclosed receipt of the following financial support for the research, authorship, and/or publication of this article: This work was supported by the National Research Foundation of Korea (NRF) grant funded by the Korean government (NSIT) (No. NRF-2022R1A2C2012470).

ORCID iD

Donghyuk Kim https://orcid.org/0000-0002-1976-1331

References

1. Liu T, Han C, Wang S, et al. Cancer-associated fibroblasts: an emerging target of anti-cancer immunotherapy. *J Hematol Oncol* 2019; 12: 86.
2. Bent EH, Millán-Barea LR, Zhuang I, et al. Microenvironmental IL-6 inhibits anti-cancer immune responses generated by cytotoxic chemotherapy. *Nat Commun* 2021; 12: 6218.
3. Deutsch E, Chargari C, Galluzzi L, et al. Optimising efficacy and reducing toxicity of anticancer radioimmunotherapy. *Lancet Oncol* 2019; 20: e452–e463.
4. Ivan ME, Eichberg DG, Di L, et al. Augmented reality head-mounted display-based incision planning in cranial neurosurgery: a prospective pilot study. *Neurosurg Focus* 2021; 51: E3.
5. Agnass P, Rodermond HM, van Veldhuisen E, et al. Quantitative analysis of contribution of mild and moderate hyperthermia to thermal ablation and sensitization of irreversible electroporation of pancreatic cancer cells. *J Therm Biol* 2023; 115: 103619.
6. Köckerling F, Simon T, Adolf D, et al. Laparoscopic IPOM versus open sublay technique for elective incisional hernia repair: a registry-based, propensity score-matched comparison of 9907 patients. *Surg Endosc* 2019; 33: 3361–3369.
7. Shen Q, Zhang X, Qi J, et al. Sinomenine hydrochloride loaded thermosensitive liposomes combined with microwave hyperthermia for the treatment of rheumatoid arthritis. *Int J Pharm* 2020; 576: 119001.
8. Mao C, Jin W, Xiang Y, et al. Reversing multidrug-resistant Escherichia coli by compromising its BAM biogenesis and enzymatic catalysis through microwave hyperthermia therapy. *Adv Funct Mater* 2022; 32: 2202887.
9. Wyllie AH. Cell death. *Cytol Cell Physiol* 1987; 17: 755–785.
10. Shamekhi L, Sayehvand HO and Karami H. Tumour shape-dependent microwave hyperthermia using a novel coaxial micro-cut slot antenna. *J Therm Biol* 2020; 88: 102473.
11. Gas P. Study on interstitial microwave hyperthermia with multi-slot coaxial antenna. *Rev Roum Sci Tech-El* 2014; 2: 215–224.
12. Selmi M, Bajahzar A and Belmabrouk H. Effects of target temperature on thermal damage during temperature-controlled MWA of liver tumor. *Case Stud Therm Eng* 2022; 31: 101821.
13. Eltigani F, Ahmed S, Yahya M, et al. Modeling of interstitial microwave hyperthermia for hepatic tumors using floating sleeve antenna. *Phys Eng Sci Med* 2022; 45: 569–575.
14. Kim D and Kim H. Induction of apoptotic temperature in photothermal therapy under various heating conditions in multi-layered skin structure. *Int J Mol Sci* 2021; 22: 11091.

15. Keangin P, Rattanadecho P and Wessapan T. An analysis of heat transfer in liver tissue during microwave ablation using single and double slot antenna. *Int Commun Heat Mass Transf* 2011; 38: 757–766.
16. Wang T, Zhao G and Qiu B. Theoretical evaluation of the treatment effectiveness of a novel coaxial multi-slot antenna for conformal microwave ablation of tumors. *Int J Heat Mass Transf* 2015; 90: 81–91.
17. Brace CL. Temperature-dependent dielectric properties of liver tissue measured during thermal ablation: toward an improved numerical model. *Annu Int Conf IEEE Eng Med Biol Soc* 2008: 230–233.
18. Wu C, Huang H, Liu Y, et al. Optimal design of aperiodic tri-slot antennas for the conformal ablation of liver tumors using an experimentally validated MWA computer model. *Comput Methods Programs Biomed* 2023; 242: 107799.
19. Deshazer G, Hagmann M, Merck D, et al. Computational modeling of 915 MHz microwave ablation: comparative assessment of temperature-dependent tissue dielectric models. *Med Phys* 2017; 44: 4859–4868.
20. O'Rourke AP, Lazebnik M, Bertram JM, et al. Dielectric properties of human normal, malignant and cirrhotic liver tissue: in vivo and ex vivo measurements from 0.5 to 20 GHz using a precision open-ended coaxial probe. *Phys Med Biol* 2007; 52: 4707.
21. Gas P. Multi-frequency analysis for interstitial microwave hyperthermia using multi-slot coaxial antenna. *J Electr Eng* 2015; 66: 26–33.
22. Rattanadecho P and Keangin P. Numerical study of heat transfer and blood flow in two-layered porous liver tissue during microwave ablation process using single and double slot antenna. *Int J Heat Mass Transf* 2013; 58: 457–470.
23. Pennes HH. Analysis of tissue and arterial blood temperatures in the resting human forearm. *J Appl Physiol* 1948; 1: 93–122.
24. Miaskowski A and Gas P. Numerical estimation of SAR and temperature distributions inside differently shaped female breast tumors during radio-frequency ablation. *Materials (Basel)* 2023; 16: 223.
25. Sturesson C and Andersson-Engels S. A mathematical model for predicting the temperature distribution in laser-induced hyperthermia. Experimental evaluation and applications. *Phys Med Biol* 1995; 40: 2037.
26. Satish V and Repaka R. Microwave ablation trocar for ablating cancerous tumors: a numerical analysis. *Med Biol Eng Comput* 2023; 61: 1113–1131.
27. Yang D, Converse MC, Mahvi DM, et al. Expanding the bioheat equation to include tissue internal water evaporation during heating. *IEEE Trans Biomed Eng* 2007; 54: 1382–1388.
28. Selmi M, Dukhyil AAB and Belmabrouk H. Numerical analysis of human cancer therapy using microwave ablation. *Appl Sci* 2019; 10: 211.
29. Tehrani MH, Soltani M, Kashkooli FM, et al. Use of microwave ablation for thermal treatment of solid tumors with different shapes and sizes—a computational approach. *PLoS One* 2020; 15: e0233219.
30. Khosravirad A and Ayani MB. Comparative analysis of thermal damage to laser-irradiated breast tumor based on Fourier conduction and non-Fourier heat conduction models: a numerical study. *Int Commun Heat Mass Transf* 2023; 145: 106837.
31. Gas P and Kurgan E. Evaluation of thermal damage of hepatic tissue during thermotherapy based on the Arrhenius model. *2018 Prog Appl Electr Eng* 2018: 1–4.

Appendix

Notation

c_0	speed of light in vacuum (m/s), $c_0 = 299{,}792{,}458$ m/s
c_p	specific heat capacity (J/kg/K)
d_m	MCA insertion depth (mm)
$\vec{E}$	electric field strength (V/m)
f	frequency (Hz)
$\vec{H}$	magnetic field strength (A/m)
k_m	thermal conductivity (W/m/K)
k_p	propagation constant (1/m)
P_{in}	microwave antenna input power (W)
r	radius (m)
t	time (s)
T	temperature (K)
Z	wave impedance (Ω)

Greek symbols

ϵ_0	vacuum permittivity (F/m), $\epsilon_0 = 8.854 \times 10^{-12}$ F/m
ϵ_r	relative permittivity
θ^*_A	apoptosis retention ratio
θ^*_{eff}	effective apoptosis retention ratio
θ^*_H	thermal hazard retention value
λ	wavelength (m)
μ	permeability (H/m)
μ_r	relative permeability
ρ	density (kg/m^3)
σ	electric conductivity (S/m)
ω	angular frequency (rad/s)
ω_b	blood perfusion rate (1/s)

Subscripts

b	blood
inner	inner
outer	outer
met	metabolism
mw	microwave
r, φ, z	coordinates
0	free space

Abbreviation

MWA	microwave ablation
MCA	microwave coaxial antenna
MCS	micro-cut slot antenna
SAR	specific absorption rate